Global Health & Medicine. 2024; 6(3):183-189.
ORIGINAL ARTICLE
DOI: 10.35772/ghm.2023.01085

Gallbladder fossa nodularity in the liver as observed in alcoholic liver disease patients: Analysis based on hepatobiliary phase signal intensity on gadoxetate-enhanced MRI and extracellular volume fraction calculated from routine CT data

Keisuke Sato[1,§], Shinji Tanaka[1,§], Hiroshi Urakawa[2], Ryo Murayama[1], Eiko Hisatomi[1], Yukihisa Takayama[1], Kengo Yoshimitsu[1,*]

[1] Department of Radiology, Faculty of Medicine, Fukuoka University, Fukuoka, Japan;
[2] Department of Radiology, Fukuoka University Chikushi Hospital, Chikushino, Japan.

Abstract: The purpose of this study is to further verify the concept utilizing signal intensity on hepatobiliary phase (HBP) of gadoxetate-enhanced MRI and extracellular volume fraction (ECV) calculated from CT data. Between Jan 2013 and September 2018, consecutive ALD patients who had both quadruple phase CT and gadoxetate-enhanced MRI within six months were retrospectively recruited. Those who had any intervention or disease involvement around gallbladder fossa were excluded. All images were reviewed and ECV was measured by two experienced radiologists. GBFN grades, and their HBP signal intensity or ECV relative to the surrounding background liver (BGL) were analyzed. There were 48 patients who met the inclusion criteria. There were GBFN grade 0/1/2/3 in 11/15/18/4 patients, respectively. The signal intensity on HBP relative to BGL were iso/slightly high/high in 30/15/3 patients, respectively, and ECV ratio (ECV of GBFN divided by that of BGL) was 0.88 ± 0.18, indicating there are more functioning hepatocytes and less fibrosis in GBFN than in BGL. The GBFN grades were significantly correlated to relative signal intensity at HBP (Spearman's rank correlation, $p < 0.01$, rho value 0.53), and ECV ratio ($p < 0.01$, rho value -0.45). Our results suggest GBFN in ALD would represent liver tissues with preserved liver function with less fibrosis, as compared to BGL, which are considered to support our hypothesis as shown above.

***Keywords*:** gallbladder fossa, nodularity, alcoholic liver disease, gadoxetate uptake, extracellular volume fraction

Introduction

Recently, it has been reported that nodularity of the gallbladder fossa (GBFN) as observed typically in patients with alcoholic liver disease (ALD) may represent spared area from portal venous perfusion containing alcohol absorbed in the gastrointestinal tract, escaped from alcohol-induced fibrotic and atrophic change of the surrounding background liver (BGL) parenchyma, due to cholecystic venous drainage (CVD) (*1-5*). Pathologically, it has been shown GBFN consists of unusually large-sized pseudo-lobules in contrast to small-sized pseudo-lobules that are known to be characteristic of alcoholic liver cirrhosis, which may as well be called "pseudo-hyperplasia" (*1,6*).

As a morphological feature of ALD-related cirrhosis as compared to those due to other etiologies, the enlargement of segment I or caudate lobe is well known (*7,8*). GBFN may serve as an adjunctive sign for ALD, with relatively high specificity but with low sensitivity, as compared to caudate lobe enlargement (*1*).

We hypothesized that, if GBFN represents relatively hyperplastic liver tissue in contrast to fibrotic BGL, gadoxetate uptake, which is a marker of functioning hepatocytes (*9-11*), at GBFN should be preserved, as compared to the surrounding fibrotic BGL, at the hepatobiliary phase (HBP) of gadoxetate-enhanced MRI (EOB-MRI). Further, we also hypothesized that the extracellular volume fraction (ECV), which has been reported to be a useful surrogate biomarker for pathological degree of liver fibrosis (*12-16*), of GBFN, should be low as compared to that of BGL. The purpose of this study is to further clarify the etiology or mechanism of GBFN, using its HBP signal intensity on EOB-MRI and ECV calculated from CT data relative to those of BGL as analytic indices.

Materials and Methods

Patients

Between January 2013 and September 2018, consecutive ALD patients who underwent both quadruple phase dynamic CT and EOB-MRI within six months in our institute were retrospectively recruited. Among those, patients who had had cholecystectomy and hepatectomy, apparent acute cholecystitis or cholangitis, hepatocellular carcinoma (HCC) involving gallbladder fossa, and tumor thrombus involving the 1st order branch or main trunk of the portal vein were excluded. Those who had any interventions around GBF, such as transarterial (chemo) embolization, radiofrequency ablation, or microwave ablation, between the two examinations, were also excluded.

Clinical diagnosis of ALD was made for patients with liver dysfunction without serological evidence of hepatitis B or C infection, or anti-mitochondrial or anti-nuclear antibodies, and with history of habitual alcohol overconsumption, based on the criteria defined by Japanese Society of Biomedical Research of Alcohol (*17*), that is, briefly, 60g /day and 40g/day or more alcohol consumption for men and women, respectively. Institutional review board approved this study and waived obtaining informed consent from the patients because of its retrospective nature (U20-02-008). Also of note is that the study was conducted in compliance with the Declaration of Helsinki.

MR protocol

MR equipment used was a 3T Discovery 750W (GE, Milwaukee, USA), and HBP images were obtained with fat saturated 3D gradient-echoT1 weighted sequences under breath-holding and that with diaphragmatic navigation, 15 min after the intravenous injection of gadoxetate (Primovist®, Bayer Health Care, Osaka, Japan). Details of the MRI protocol are shown in Supplemental Table S1 (*https://www.globalhealthmedicine.com/site/supplementaldata.html?ID=78*).

CT protocol

Two CT instruments were used in this study. One was an area-detector CT (Aquilion ONE ViSION Edition, Canon Medical Systems, Tokyo, Japan), and scanning parameters were as follows: 0.5 mm × 80 row, 120 kVp, three-dimensional auto-exposure control (Volume EC: SD12@5 mm), 0.5 sec/rotation, 0.813 beam pitch, 512 × 512 matrix, 300–350 mm field-of-view, and 2 mm reconstruction. Noise reduction was achieved using a hybrid iterative reconstruction (ADIR 3D Weak). The other CT used was 64-row multi-detector CT (Aquilion 64, Canon Medical Systems, Tokyo, Japan), with parameters shown below: 0.5 mm × 64 row, 120 kVp, three-dimensional auto-exposure control (Volume EC: SD12@5 mm), 0.5 sec/rotation, 0.828 beam pitch, 512 × 512 matrix, 300–350 mm field-of-view, and 2mm reconstruction (filtered back projection). Portal venous phase was additionally reconstructed along the coronal plane with 2 mm contiguous slice thickness in either CT.

After obtaining unenhanced images, 600 mg/kg iodine contrast medium (Iopamiron 370, Bayer Health Care, Osaka, Japan) was injected for 30 sec at a variable injection rate, and arterial dominant phase images were obtained using a bolus tracking method, followed by portal dominant phase at 60 sec, and equilibrium phase images at 240 sec after the commencement of contrast medium injection.

ECV map generation

ECV map was generated from pre-contrast and equilibrium phase CT data, according to the previously reported method (*14-16*). Just briefly, because ECV is defined as (100- hematocrit) * Δ liver /Δ blood pool, where Δ represents the difference in the CT values between the unenhanced and equilibrium phase (*12-16*), ECV map was generated on the dedicated workstation by means of subtracting unenhanced images from equilibrium phase images utilizing a non-linear non-rigid anatomical correction algorithm, and inputting the hematocrit value for each patient (*14-16*).

Assessment

All qualitative assessments were performed by two radiologists (KS and ST) independently first, and disagreement was resolved by consensus. The grades of GBFN were assessed, separately for CT and MRI, according to the definitions as previously reported (*1*): just briefly, grade 0 represents flat surface of the gallbladder fossa (GBF) without notch or protrusion; grade 1, minimal protrusion with slight notch at GBF; grade 2, slight protrusion with notches, the degree of which is between grade 1 and grade 3; grade 3, apparent nodularity of GBF. After determining GBFN grades, the two radiologists independently assessed HBP signal intensity of GBFN relative to BGL both on axial and coronal images, and higher signal on either plane was adopted to represent the patient. The quantitative assessment, namely, ECV measurement, was performed by the same two radiologists (KS and ST) independently for the first 20 patients to assess inter-observer agreement. One radiologist (KS) performed ECV measurement for the rest of the patients. ECV was measured by placing as large an oval-shaped region-of-interest (ROI) as possible on ECV map as generated from pre-contrast and equilibrium phase CT data, as previously reported (*14-16*). As for GBFN EVC measurement, ROI was placed in its center. As for ECV

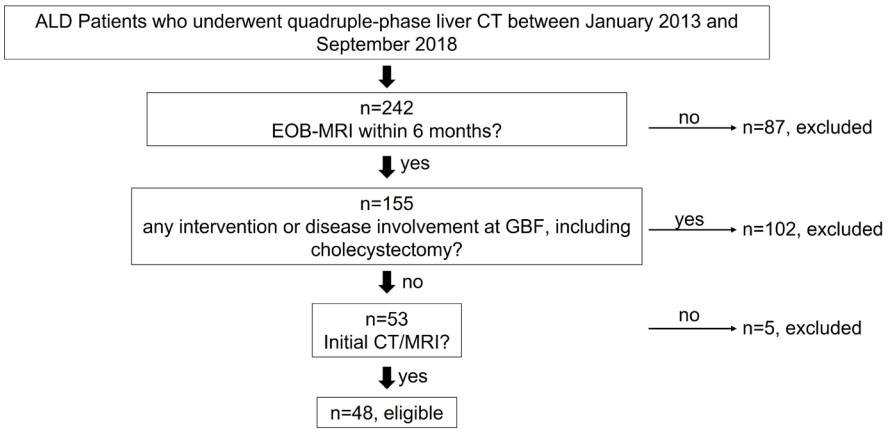

Figure 1. Patient inclusion flow chart. ALD: alcoholic liver disease, EOB-MRI: gadoxetate-enhanced MRI, GBF: gallbladder fossa.

measurement for BGL, ROIs were placed in the anterior, posterior, and medial segments, because these three segments were considered to be anatomically closely related to gallbladder fossa; and their averaged value was used to represent ECV of BGL. For the anterior and medial segment measurement, the axial slice slightly cephalad to GBFN was selected where both middle hepatic vein and the anterior branch of portal vein were clearly visualized. For posterior segment measurement, the same slice as GBFN visualized was selected, and ROIs were carefully placed avoiding apparent vessels, masses or artifacts. The ECV of GBFN divided by that of BGL was defined as ECV ratio. The grades of HBP signal intensity and ECV ratio were correlated to modified albumin-bilirubin (mALBI) grades (*18,19*), which is an indicator of liver function in CLD patients. Blood sample data were selected from the date, which was closest to that of CT for mALBI assessment and ECV calculation.

Statistics

Inter-observer concordance for qualitative assessment was assessed with kappa statistics, and that for quantitative assessment, namely, ECV, was evaluated by intra-class coefficient (ICC). Univariable analysis was performed with *t*-test, Fisher's exact probability test, or Tukey-Kramer's HSD test for parametric variables, and with Mann-Whitney test, or Wilcoxon's rank test, for non-parametric variables. Correlation for non-parametric variables was assessed using Spearman's rank correlation test. *P* values less than 0.05 were considered statistically significant. All statistical analyses were performed using JMP Pro13.0.0 (SAS corporation, Cary, USA).

Results

Patients

Patient selection flow chart is shown in Figure 1. There were 48 patients for whom both CT and MRI were obtained within six months, without history of any intervention around the gallbladder fossa. Among these, 5 patients had two sets of CT and MRI, for whom the initial set was adopted for this study. There were 43 men and 5 women, with an average age of 60.6 years. Of the 48 patients, 41 were included in the previous study (*1*). Details of the demographic data of the patients are shown in Table 1. The interval between CT and blood sampling was 3.2 ± 4.3 days (range 0–20).

Table 1. Demographic data and GBFN information of 48 ALD patients

Characteristic	Values
Age	60.6 ± 10.9 (range 28-83)
Sex	M:F = 43:5
mALBI grade	1/ 2a/ 2b/ 3 = 14/ 9/ 2/ 3
CP grade/score	A5/ A6/ B7/ B8/ B9 /C10 = 20/ 14/ 5/ 4/ 4/ 1
GBFN grade	0/ 1/ 2/ 3 = 11/ 15/ 8/ 4
HBP signal intensity	Iso/ slightly high/ high = 30/ 15/ 3
ECV of GBFN	31.5 ± 7.7 (range 14.6 – 50.4)
ECV of BGL	36.4 ± 7.8 (range 22.6 – 53.2)
ECV ratio	0.88 ± 0.18 (range 0.53 – 1.36)

ALD: alcoholic liver disease, M/F: male/female, mALBI: modified albumin-bilirubin, CP: Child-Pugh, GBFN: gallbladder fossa nodularity, HBP: hepatobiliary phase, ECV: extracellular volume fraction, BGL: background liver, P/N: positive/negative.

GBFN and related factors assessment

Kappa value for the two radiologists in assessing the grades of GBFN was 0.68, showing good agreement. That for signal intensity of GBFN on HBP was 0.85, showing excellent agreement. Final GBFN grades were identical for CT and MRI.

There was a weak, but significantly positive correlation between GBFN grades and mALBI grades (Spearman's rank correlation, $p < 0.05$, rho value 0.34), namely, the higher the grades of GBFN, the higher mALBI grade is (more severely impaired liver function) (Table 2). HBP signal intensities of GBFN

Table 2. Correlation between GBFN grades and modified ALBI grades

Items	mALBI				Total
	Grade 1	Grade 2a	Grade 2b	Grade 3	
GBFN					
Grade 0	8	0	3	0	11
Grade 1	4	3	7	1	15
Grade 2	1	4	11	2	18
Grade 3	1	2	1	0	4
Total	14	9	22	3	48

There was a significantly positive correlation between GBFN grades and ALBI grades (Spearman's rank correlation, $p < 0.05$, rho value 0.34). GBFN: gallbladder fossa nodularity, mALBI: modified Albumin-Bilirubin grade.

Table 3. Correlation between GBFN grades and HBP signal intensity relative to surrounding BGL on gadoxetate-enhanced MRI

Items	HBP signal intensity relative to BGL			Total
	Iso	slightly high	high	
GBFN				
Grade 0	11	0	0	11
Grade 1	12	3	0	15
Grade 2	6	10	2	18
Grade 3	1	2	1	4
Total	30	15	3	48

There was a moderately positive correlation between GBFN grades and HBP signal intensity relative to BGL (Spearman's rank correlation, $p = 0.003$, rho value 0.53). GBFN: gallbladder fossa nodularity, HBP: hepatobiliary phase, BGL: background liver.

relative to BGL were iso, slightly high, and high, in 30, 15, and 3 patients, respectively. There was a moderate and significantly positive correlation between grades of GBFN and HBP signal intensity relative to BGL (Spearman's rank correlation, $p < 0.001$, rho value 0.53), namely, the higher the GBFN grade, the higher HBP signal intensity relative to BGL (Table 3).

As for ECV measurement, ECV of GBFN was 31.7 ± 10.1 for observer 1, and 29.8 ± 13.3 for observer 2, showing ICC of 0.87, whereas ECV of BGL (average of three segments) was 36.6 ± 10.3 for observer 1, and 38.0 ± 14.1 for observer 2, with an ICC of 0.75, both showing good agreement, for the first 20 patients. ECV ratio was 0.88 ± 0.18 for all 48 patients, suggesting there is less fibrotic tissue in GBFN as compared to BGL. Paired *t*-test also showed there is a significant difference between ECV of GBFN and that of BGL ($p < 0.0001$). There was a strong, significantly negative correlation between GBFN grades and ECV ratio (Spearman's rank correlation, $p < 0.01$, rho value -0.45), namely, the higher the GBFN grade, the lower the ECV ratio (Figure 2).

Lastly, we additionally assessed the correlation between ECV ratio and HBP signal intensity, which showed significant correlation (Figure 3, Spearman's rank correlation, $p < 0.01$, rho value -0.42).

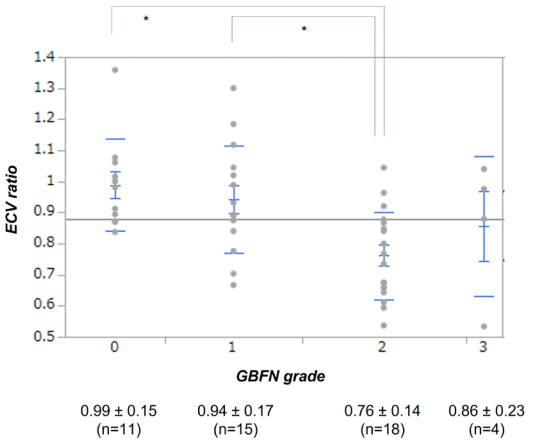

Figure 2. Correlation between gallbladder fossa nodularity (GBFN) grades and extracellular volume fraction (ECV) ratio. There was a statistically significant difference (*) in ECV ratio between GBFN grades 0 and 2 (Tukey-Kramer's HSD test, $p = 0.0032$), and between grades 1 and 2 ($p = 0.013$). Spearman's rank correlation suggested significantly negative correlation between GBFN grades and ECV ratio ($p = 0.0013$, rho value -0.452).

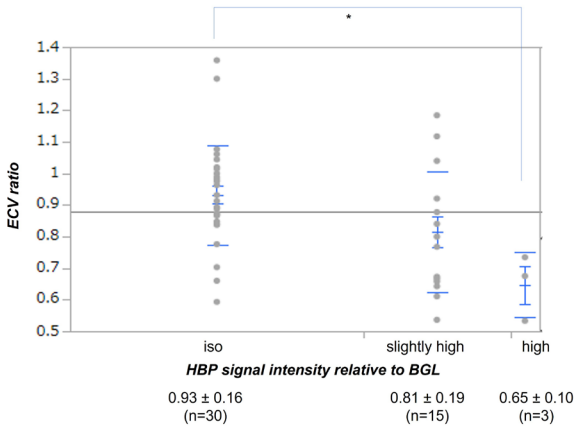

Figure 3. Correlation between extracellular volume fraction (ECV) ratio and hepatobiliary phase (HBP) signal intensity relative to surrounding background liver (BGL) on gadoxetate-enhanced MRI. There was a statistically significant difference (*) in ECV ratio between iso-intensity and high intensity (Tukey-Kramer's HSD test, $p = 0.019$). Spearman's rank correlation suggested significantly negative correlation between ECV ratio and HBP signal intensity ($p = 0.0027$, rho value -0.424).

Representative cases are shown in Figures 4–6, all of whom show similar to higher signal intensity of GBFN as compared to background liver, and ECV ratio of around 0.6.

Discussion

In this study, we tried to further verify our hypothesis that GBFN typically observed in ALD patients may represent "pseudo-hyperplastic" liver parenchyma around GBF, escaping from alcohol containing portal perfusion due to cholecystic venous drainage (*1,6*), from viewpoints

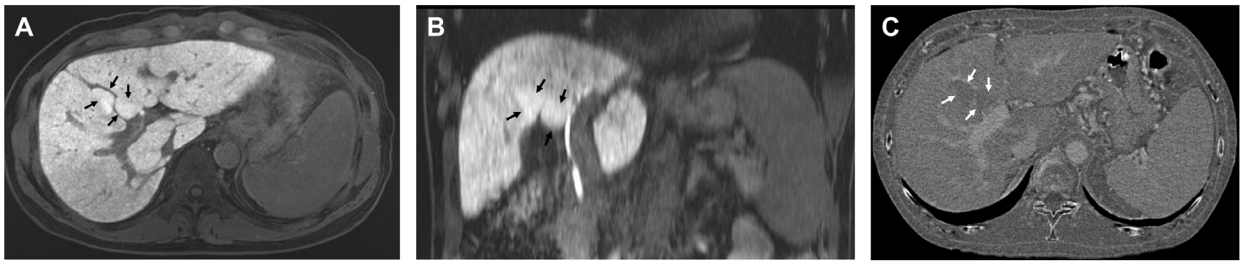

Figure 4. A 47-year-old man with alcoholic liver disease (ALD). Child-Pugh grade/score was A/6, and modified albumin-bilirubin grade/score was 2a/-2.5. An apparent nodularity (arrows) is observed at the gallbladder fossa (GBF) around the neck. GBF nodularity grade 3 was assigned. **(A)** Hepatobiliary phase axial image of gadoxetate-enhanced MRI. GBFN exhibits slightly higher signal intensity (arrows) than the surrounding background liver. **(B)** Oblique coronal reconstruction image of hepatobiliary phase of gadoxeate-enhanced MRI. GBFN exhibits slightly higher signal intensity than the surrounding background liver (arrows). **(C)** Extracellular volume fraction (ECV) map calculated from CT obtained 3 months before MRI through the slice corresponding to 4**A**. ECV of GBFN (arrows) was 20%, whereas that of background liver ECV (average of anterior, posterior, and medial segments, not shown) was 30%. ECV ratio was 0.67. Note GBFN of apparent low ECV value (arrows).

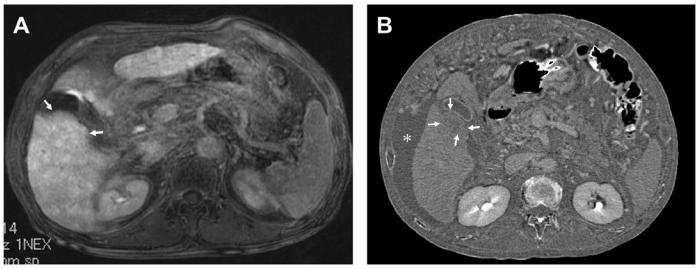

Figure 5. A 61-year-old man with alcoholic liver disease (ALD). Child-Pugh grade/score was A/5, and modified albumin-bilirubin grade/score was 1/-3.0. A slight nodularity (arrows) is appreciable at the gallbladder fossa (GBF). GBF nodularity grade 2 was assigned. **(A)** Hepatobiliary phase image of gadoxetate-enhanced MRI. GBFN exhibits almost similar signal intensity as the surrounding background liver (arrows). **(B)** Extracellular volume fraction (ECV) map calculated from CT obtained 4 months after MRI. There is apparent increase in the volume of ascites (*) as compared to 5**A**. ECV of GBFN was 26%, whereas that of background liver (average of anterior, posterior, and medial segments, not shown) was 45%. ECV ratio was 0.59. Note GBFN of apparent low ECV value (arrows).

Figure 6. A 60-year-old woman with alcoholic liver disease. Child-Pugh grade/score was A/5, and modified albumin-bilirubin grade/score was 2/-2.0. A faint nodularity (arrows) is appreciable at the gallbladder fossa (GBF). GBF nodularity grade 1 was assigned. **(A)** Hepatobiliary phase image of gadoxetate-enhanced MRI. GBFN exhibits higher signal intensity than the surrounding background liver. **(B)** Extracellular volume fraction (ECV) map calculated from CT obtained 3 months before MRI. ECV of GBFN was 27%, whereas that of background liver (average of anterior, posterior, and medial segments, not shown) was 44%. ECV ratio was 0.61. Note GBFN of apparent low ECV value (arrows). **(C)** Unenhanced CT for anatomical correlation of GBFN with 6**B**.

of HBP signal intensity on EOB-MR and ECV obtained from routine CT data.

Gadoxetate is a hepatocyte-specific contrast agent, taken up *via* organic anion-transporting polypeptide (OATP) as expressed on the cellular membrane of hepatocytes, and it has been known that in patients with liver dysfunction or liver cirrhosis, parenchymal enhancement decreases, typically at the HBP images of EOB-MRI, along with decreased expression of OATP (*11*). Our results that HBP signal intensity of GBFN was similar to (two thirds) or higher (one third) than that of BGL, and also that its grade was positively correlated to GBFN grades, would support the above-mentioned hypothesis.

ECV of the liver has drawn attention as a biomarker of pathological grades of liver fibrosis (*12-16*). ECV is

a sum of intravascular and extravascular extracellular spaces, which can be easily calculated from non-contrast and equilibrium phase CT data of routine clinical practice, because the concentration of iodine is considered the same for both intravascular and extravascular spaces at the equilibrium phase (*12-16*). We have reported the usefulness of ECV map, which is generated by subtracting precontrast images from equilibrium phase images utilizing a non-linear non-rigid anatomical correction algorithm specifically adjusted to upper abdominal organs (*14-16*), and promising results have been obtained for the estimation of degree of liver fibrosis (*14*). Thanks to the highly accurate subtraction algorithm, the anatomical misregistration is minimized in this ECV map, and therefore precise ECV can be obtained for any small area of any part of the liver (*16*), like GBFN. Our results that ECV of GBFN is significantly less than that of BGL, along with overall ECV ratio being less than 1 (0.88), and GBFN grades negatively correlated to ECV ratio, would also support the above-mentioned hypothesis.

Our results suggested GBFN is characterized by relatively higher signal intensity on HBP and less ECV as compared to the surrounding BGL, indicating that areas of GBFN is closer to normal liver tissue as compared to the BGL affected by alcohol. This knowledge would help radiologists understand the morpho-radiological features of the liver in CLD patients, particularly those with ALD.

There are several limitations of this study. Due to its retrospective nature, there could be a bias in patient selection. That this is a single arm study dealing with only ALD patients without any control cohort to compare, could be another limitation. Because the previous study (*1*) showed GBFN of mild grades (up to grade 2) can be observed in chronic hepatitis C patients as well, although less frequently than in ALD patients, we focused on an ALD patient cohort in this study to make it easier to clarify the characteristic features in HBP signal intensity and ECV values. It is possible that GBFN in patients with CLD of other etiologies may show different tendencies, which should be clarified in future studies. Lack of pathological proof in any of our study population is another limitation, however, it would be ethically difficult to justify obtaining histological specimens of GBFN in ALD patients. Furthermore, as mentioned earlier, there is a recent pathological investigation (*6*) confirming the presence of GBFN as a pseudo-hyperplastic change in autopsy ALD cases, which would be sufficient as a pathological support for our hypothesis. Finally, the subjective way of assessing the grades of GBFN and HBP signal intensity, or manual ECV measurement, may be included as a limitation, however, the kappa values or ICC in our study suggested agreements between the two radiologists were reasonably high.

In conclusion, GBFN tends to show higher HBP signal intensity on EOB-MRI and lower ECV calculated from CT data as compared to the surrounding BGL, which is considered to support the hypothesis that GBFN is "pseudo-hyperplastic" liver parenchyma around gallbladder fossa, escaping from alcohol-containing portal venous perfusion due to CVD.

Acknowledgements

Authors greatly thank Professor Fumihito Hirai, Department of Gastroenterology, Faculty of Medicine, Fukuoka University, and also Professor Suguru Hasegawa, Department of Gastroenterological Surgery, for providing patients' clinical information.

Funding: None.

Conflict of Interest: The authors have no conflicts of interest to disclose.

References

1. Tanaka S, Sato K, Yamamoto R, Urakawa H, Ito E, Takayama Y, Yoshimitsu K. Gallbladder fossa nodularity typically observed in patients with alcoholic liver disease: comparison with chronic hepatitis C patients. Abdom Radiol (NY). 2023; 48:1965-1974.
2. Yoshimitsu K, Honda H, Kaneko K, Kuroiwa T, Irie H, Chijiiwa K, Takenaka K, Masuda K. Anatomy and clinical importance of cholecystic venous drainage: Helical CT observations during injection of contrast medium into the cholecystic artery. AJR Am J Roentgenol. 1997; 169:505-510.
3. Yoshimitsu K, Honda H, Kuroiwa T, Irie H, Aibe H, Shinozaki K, Masuda K. Unusual hemodynamics and pseudolesions of the noncirrhotic liver at CT. Radiographics. 2001; 21 Spec No:S81-S96.
4. Yoshimitsu K, Irie H, Aibe H, Tajima T, Nishie A, Asayama Y, Matake K, Nakayamka T, Kakihara D, Honda H. Pitfalls in the imaging diagnosis of hepatocellular nodules in the cirrhotic and noncirrhotic liver. Intervirology. 2004; 47:238-251.
5. Yoshimitsu K, Honda H, Kuroiwa T, Irie H, Aibe H, Tajima T, Chijiiwa K, Shimada M, Masuda K. Liver metastasis from gallbladder carcinoma: anatomic correlation with cholecystic venous drainage demonstrated by helical computed tomography during injection of contrast medium in the cholecystic artery. Cancer. 2001; 92:340-348.
6. Nakano M. Gallbladder fossa nodules in patients with alcoholic cirrhosis. Proceedings of The 26th Meeting of Association of Hemodynamic and Functional Image of the Liver. 2020; Kanazawa, Japan. (in Japanese)
7. Okazaki H, Ito K, Fujita T, Koike S, Takano K, Matsunaga N. Discrimination of alcoholic from virus-induced cirrhosis on MR imaging. AJR Am J Roentgenol. 2000; 175:1677-1681.
8. Ito K, Mitchell DG. Imaging diagnosis of cirrhosis and chronic hepatitis. Intervirology. 2004; 47:134-143.
9. Yamada A, Hara T, Li F, Fujinaga Y, Ueda K, Kadoya M, Doi K. Quantitative evaluation of liver function with use of gadoxetate disodium- enhanced MR imaging. Radiology. 2011; 260:727-733.

10. Yasaka K, Akai H, Kunimatsu A, Abe O, Kiryu S. Liver fibrosis: Deep convolutional neural network for staging by using gadoxetic acid–enhanced hepatobiliary phase MR images. Radiology. 2018; 287:146-156.
11. Noda Y, Goshima S, Okuaki T, Akamine Y, Kajita K, Kawai N, Kawada H, Tanahashi Y, Matsuo M. Hepatocyte fraction: Correlation with noninvasive liver functional biomarkers. Abdom Radiol (NY). 2020; 45:83-89.
12. Varenika V, Fu Y, Maher JJ, Gao D, Kakar S, Cabarrus MC, Yeh BM. Hepatic fibrosis: evaluation with semiquantitative contrast-enhanced CT. Radiology. 2013; 266:151-158.
13. Bandula S, Punwani S, Rosenberg WM, Jalan R, Hall AR, Dhillon A, Moon JC, Taylor SA. Equilibrium contrast-enhanced CT imaging to evaluate hepatic fibrosis: Initial validation by comparison with histopathologic analysis. Radiology. 2015; 275:136-143.
14. Shinagawa Y, Sakamoto K, Sato K, Ito E, Urakawa H, Yoshimitsu K. Usefulness of new subtraction algorithm in estimating degree of liver fibrosis by calculating extracellular volume fraction obtained from routine liver CT protocol equilibrium phase data: Preliminary experience. Eur J Radiol. 2018; 103:99-104.
15. Tani T, Sato K, Sakamoto K, Ito E, Nishiyama M, Urakawa H, Yoshimitsu K. Importance of extracellular volume fraction of the spleen as a predictive biomarker for high-risk esophago-gastric varices in patients with chronic liver diseases: A preliminary report. Eur J Radiol. 2021; 143:109924.
16. Sakamoto K, Tanaka S, Sato K, Ito E, Nishiyama M, Urakawa H, Arima H, Yoshimitsu K. What is the "washout" of hepatocellular carcinoma as observed on the equilibrium phase CT?: consideration based on the concept of extracellular volume fraction. Jpn J Radiol. 2022; 40:1148-1155.
17. National Center for Global Health and Medicine. *http://www.kanen.ncgm.go.jp/cont/010/sankou.html* (assessed June 20, 2023). (in Japanese)
18. Johnson PJ, Berhane S, Kagebayashi C, *et al.* Assessment of liver function in patients with hepatocellular carcinoma: A new evidence-based approach - the ALBI grade. J Clin Oncol. 2015; 33:550-558.
19. Hiraoka A, Kumada T, Tsuji K, *et al.* Validation of modified ALBI grade for more detailed assessment of hepatic function in hepatocellular carcinoma patients: A multicenter analysis. Liver Cancer. 2019; 8:121-129.

Received August 6, 2023; Revised December 25, 2023; Accepted January 29, 2024.

Released online in J-STAGE as advance publication March 15, 2024.

[§]*These authors contributed equally to this work.*
**Address correspondence to*:
Kengo Yoshimitsu, Department of Radiology, Faculty of Medicine, Fukuoka University, 7-45-1 Nanakuma Jonan-ku, Fukuoka City 814-0180, Japan.
E-mail: kengo@fukuoka-u.ac.jp